

DFT STUDY OF H₂ COMBUSTION ON α -Al₂O₃ SUPPORTED Pt CLUSTERS

J. Synowczynski*, J. Andzelm
U. S. Army Research Laboratory
Aberdeen Proving Grounds, MD 21005

D. G. Vlachos
University of Delaware
Newark, DE 19716-3110

ABSTRACT

Based on Density Functional Theory – Generalized Gradient Approximation calculations (DFT-GGA), we provide a theoretical model for the H₂ combustion on Al₂O₃ supported catalytically active Pt nanoclusters. In a previous paper (Synowczynski, 2008), we identified several adsorption and dissociation processes that occur on the Al₂O₃ support and demonstrated that products from these reactions can migrate along the Al₂O₃ surface. In this paper, we build on this model to show how these products influence catalytic activity at the Pt particle. We also identify new reactant structures that are unique to the Pt/Al₂O₃ interface. These processes are key to understanding the ‘inverse spillover effect’ and the influence of the Pt/Al₂O₃ interface during hydrogen combustion on alumina surfaces.

1. INTRODUCTION

As the electronics behind the future warrior systems become more sophisticated, the weight of the batteries is an ever-increasing burden. One solution is to create a compact micro-burner device as shown in Figure 1 (Norton et al., 2004) that combusts a higher energy density fuel such as methane (energy density = 3053 W-hr/kg compared to 125 W-hr/kg for Li-ion batteries) and converts the released enthalpy into electrical power. The barrier to implementing this technology on the battlefield has been maintaining the flame stability. In confined reactors (i.e. smaller than a few millimeters), the physics is very different from the physics of conventional flames used in macroscopic power generation devices. Flames are unstable due to an increase in both the free radical and thermal quenching at the reactor walls (Miesse, 2004). Both dissipation mechanisms increase in confined systems due to the increase in the surface to volume ratio. Maintaining flame stability under these conditions using conventional, homogeneous combustion (flame combustion) requires high operating temperatures (> 1000°C) which are difficult to implement in a compact device. In contrast, catalytic combustion can be performed with high efficiency in sub-mm geometries at temperatures as low as 100°C using a variety of fuels.

Although there are many computational studies which detail the complete reaction mechanism for reactant and product species interacting with the catalytically active cluster, few consider the effect of the Al₂O₃ support. New reaction pathways can arise due to support surface termination. One example of such a pathway is the “inverse spillover effect” (ISE) which occurs when H₂O chemisorbs or dissociates on the support forming mobile species that can migrate to the catalytically active particle and further promote combustion. Experimental evidence for ISE comes from the work of Wang et al. 1996 who demonstrated that CO can liberate H₂ from H₂O bound to Al₂O₃ support. Also of interest is the Pt / Al₂O₃ interface. Theoretical and experimental studies (Ogawa, 1995, Kulawik, 2006, Frondelius, 2008, Hellman, 2008) have shown that charge transfer from the Al₂O₃ support to the metal can induce large structural relaxations at the interface and change the polarity of the metal. In addition, the accumulation of charge on adsorbents such as NO₂ can create a charge depletion at the oxide-metal interface and subsequently polarize the oxide surface. A complete model of H₂ micro-combustion must encompass all of these effects.

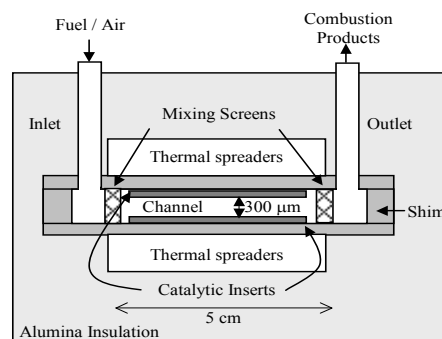


Figure 1: Microburner Schematic; Note: catalytic insert consists of nanosized Pt dispersed within porous Al₂O₃

2. PREVIOUS WORK

In our previous paper (Synowczynski, 2008), we performed a theoretical investigation of reaction processes that occurred on the alumina support during H₂ combustion. Our model suggested that H₂O is a primary source of mobile oxygen and hydrogen species. Although

O₂ can adsorb molecularly, it cannot further dissociate to create mobile oxygen. However, H can diffuse away from dissociated water leaving behind an Al^{III}-OH hydroxyl which can also further dissociate creating a O-H pair. The dissociated O-H pair can diffuse with a barrier ~24 kcal/mol. We also found that H₂ dissociation is an active source of mobile H species.

In this paper, we identify the pathways by which these dissociation products diffuse to the Pt particle and participate in catalytically activated H₂ combustion. We also discuss the changes in α -Al₂O₃ (0001) surface

3. MODEL PARAMETERS AND VALIDATION

3.1 α -Al₂O₃ Surface Termination

Our model (see Figure 2) consisted of a nine atomic layer thick Al terminated (0001) slab that is repeated under periodic boundary conditions as a 2x2 supercell with P1 symmetry and a 30Å vacuum layer to prevent any interaction between periodic images. We chose this surface based on the availability of experimental and theoretical data in the literature as well as the work of Marmier et al., 2004 who calculated surface phase diagrams as a function of temperature and the O and H partial pressures for several different crystal orientations and surface terminations. The lattice parameters for the rhombohedral unit cell ($a=b=4.749$ Å, $c=12.991$ Å) were taken directly from experimental results (Swansen, 1960) and were not optimized during the simulation. In addition, we constrained the bottom two layers of the slab to reflect the bulk Al₂O₃ geometry.

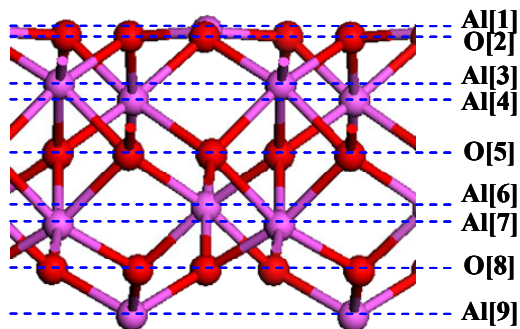


Figure 2: Cross section of fully relaxed Al terminated α -Al₂O₃ (0001) slab used for calculation. Oxygen and aluminum atoms are red and magenta respectively.

3.2 Model Parameters

All calculations were performed using ideal conditions (0 K, ultra high vacuum, defect free surface). The calculations were executed within the DMol³ (Delley, 2000) module of the Materials Studio (version 4) software package using a double-numeric basis set with

polarization functions (DNP) and the Perdew-Burke-Ernzerhof (PBE-Perdew, 1996) version of the generalized gradient approximation (GGA-) to represent the electron exchange and correlations. The ion cores were described by a density functional semi-core pseudopotential (DSPP-Delley, 2002).

To validate our calculations, we compare our results for the surface reconstruction of the relaxed α -Al₂O₃ (0001) slab with the results of other theoretical and experimental investigations (see Table 1). In agreement with other theoretical studies, our simulation predicts an 89% contraction of the inter-atomic spacing of top surface layer and 6% expansion of the first sub-layer for the ultra-clean α -Al₂O₃ (0001) surface. The predicted surface reconstruction was explained by Sousa et al. 1993 as a result of charge redistribution due to the highly ionic nature of alumina. The experimental value for this relaxation is closer to ~50%. The discrepancy between theoretical prediction and experimental measurements may be due to the difficulty in preparing a perfectly terminated surface with no adsorbed atoms or defects.

To simulate adsorption phenomena, we added one adsorbate molecule per supercell which is equivalent to approximately 1/12 monolayer according to Verdozzi et al. 1999 who define a monolayer as having one metal atom per surface oxygen. Binding energies were computed by subtracting the energy of the clean fully

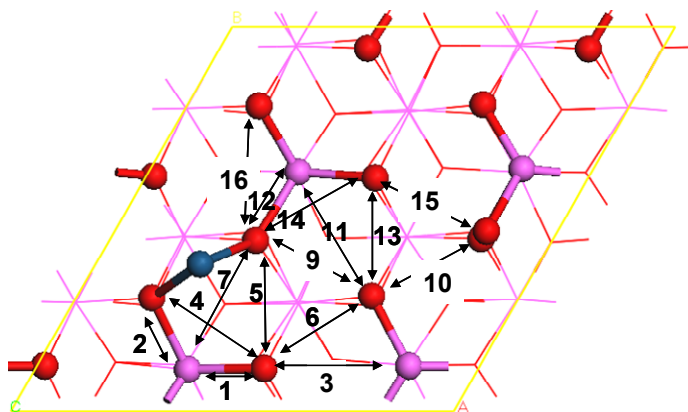


Figure 3: Top view of a 2x2 supercell showing allowed surface binding sites. The numbers correlate with the product structure and diffusion path notation referred to throughout the paper. For Pt product structures the arrow endpoints indicate surface atoms to which Pt binds. For diffusion calculations, the blue atom denotes the position of Pt in the reactant structure and the arrow endpoints refer to the oxygen position in the reactant and product structures. The Pt position changes slightly for paths 5, 7, 9, 4, 14, 16 as the diffusing oxygen forms new product structures with Pt. All barrier calculations are performed for O diffusing towards the Pt particle.

Table 1: Comparison of Theoretical and Experimentally Measured Changes in the Inter-atomic Layer Spacing of Al Terminated $\alpha\text{Al}_2\text{O}_3$ (0001) Slab with respect to their Unrelaxed Geometry

	Theoretical							Experimental	
	Ours	Hinneman	Verdozzi	Hass	Alavi	Ruberto	Carrasco	Guenard	Ahn
#Oxygen layers	3	9	18	3	3	9	11		
Functional	PBE/DSPP	PBE/PAW	LDA/NCPP	PBE/NCPP	PW91/USPP	PW91/NCPP	PBE/PAW		
Al ^[1] -O ^[2]	-89.2	-86.4	-87.4	-98	-97	-85.5	-93.8	-51	63
O ^[2] -Al ^[3]	+6	+4	+3.1	+5	+2	+3.2	+6.1	+16	
Al ^[3] -Al ^[4]	-39.9	-45.4	-41.7	-48	-53	-45.4	-46.7	-29	
Al ^[4] -O ^[5]	+18.9	+20.5	+18.3	+21	-27	+19.8	+22.0	+20	
O ^[5] -Al ^[6]	+17.1	+5	+5.6			+4.8	+8.5		
Al ^[6] -Al ^[7]	-31.2	-6.8	-8.3			-7.1	-11.6		
Al ^[7] -O ^[8]	0	+1.3	+1.1			+1.3	+2.2		
O ^[8] -Al ^[9]	0	-1.3	-0.5			-0.8	+0.7		
Al ^[9] -Al ^[10]		+4.6	+6.4			+3.0	+3.8		
Al ^[10] -O ^[11]		-1.2	-0.6			-0.7	-3.2		

relaxed slab and the adsorbent molecule (Pt, H₂O, O₂, H₂) from the total energy of the system after adsorption. We performed barrier calculations for the surface diffusion of O towards the catalytically active Pt particle using the linear synchronous transit (LST) method of Govind et al, 2003 to extrapolate between reactant and product structures along the diffusion pathways illustrated in Figure 3.

3.3 Electron Spin State

The reaction chemistry of oxygen involved reactions on Al₂O₃ surfaces cannot be adequately described without careful consideration of the triplet- to-singlet spin conversion that occurs when the $2p\pi_g^*$ orbitals hybridize with the surface states. We find the energy difference between the triplet and the singlet ground state of free O₂ to be 19.3 kcal/mol which is in good agreement with the experimentally measured value of 22.6 kcal/mol (Herzberg, 1950). Figure 4 shows adsorption structures and dissociation products for O, H, O₂, H₂, and H₂O on the Al terminated - $\alpha\text{Al}_2\text{O}_3$ (0001) surface. For all adsorption / dissociation products except Figure 4A, 4E, and 4J, the lowest energy spin state was singlet. In Table 2, we detail the key molecular features for these structures as well as their binding energies. From Table 2, it is clear that triplet states result in tighter O=O bonds and a local elongation of the Al^[1] - O bonding scheme. The spin state has no apparent effect on the length of hydroxyl or Al^[1]-H^[ads] bonds. The triplet to singlet spin conversion occurs between 2 and 1.9Å above the surface for molecular O₂ and between 1.8 and 1.5 Å for atomic oxygen.

Since an objective of this research is to establish how dissociated O from the alumina support diffuses to the catalytic particle and all possible surface diffusion pathways include a bridging conformation, we chose to

Table 2: Effect of Spin State on O₂ Adsorption Binding Energies and Bond Lengths. The ID notation refers to the structures in Figure 4.

Atomic Oxygen Adsorption				
	E _{binding} (kcal/mol) [Gamallo, 2007]	O ^[ads] -O ^[2] (Å)	O ^[ads] -Al ^[1] (Å)	∠ _{bond} (degrees)
Triplet A	[-42]	-----	1.782	112
Singlet A	-30 [-35]	-----	1.767	115
Triplet B	[-18]	1.508	1.797	49
Singlet B	-49 [-53]	1.546	1.803	50
Atomic Hydrogen Adsorption				
	E _{binding}	H ^[ads] -O ^[2]	H ^[ads] -Al ^[1]	∠ _{bond}
Triplet C	-20	-----	1.626	114
Singlet C	-36	-----	1.625	114
Triplet D	-98	0.971	-----	124
Singlet D	-116	0.972	-----	124
Molecular Oxygen Adsorption / Dissociation				
	E _{binding}	O=O	O ^[ads] -Al ^[1]	∠ _{bond}
Triplet E	-7	1.255	1.997	107
Singlet E	-13	1.276	1.959	110
Triplet F	21	1.364	1.895	74
Singlet F	-3	1.393	1.851	76
Triplet G	51	1.499	1.837	48
Singlet G	25	1.522	1.823	49
Molecular Hydrogen Dissociation				
	E _{binding}	H ^[ads] -O ^[2]	H ^[ads] -Al ^[1]	∠ _{bond} OH,HOAl
Triplet H	-15	0.982	1.594	110, 120
Singlet H	-14	0.981	1.593	110, 120
Triplet I	-14	0.971	1.621	120, 113
Singlet I	-10	0.972	1.615	121, 112
Triplet J	-85	0.973	-----	127, ----
Singlet J	-67	0.973	-----	127, ----

Table 2 continued.

H ₂ O Adsorption / Dissociation				
	E _{binding} [Hass, 2000]	H ^[ads] -O ^[2]	O ^[ads] -Al ^[1]	∠OAlO OH, OAlO
Triplet K	-27 [-23]	0.982	1.982	----, 87
Singlet K	-26 [-23]	0.983	1.987	----, 86
Triplet L	-40 [-33]	0.982	1.740	110, 112
Singlet L	-38 [-33]	0.981	1.740	109, 114
Triplet M	-38 [-33]	0.972	1.759	121, 97
Singlet M	-34 [-33]	0.973	1.758	122, 97

perform our barrier calculations using a singlet spin state for both the reactant and products. This is the most accurate method to explore the effects of crystal symmetry and surface reconstructions on the dissociation and diffusion barriers for reaction pathways that do not involve a spin change. In future studies, we will perform a detailed sampling of both the triplet and singlet potential energy surfaces using the constrained geometry method to assess the reaction barriers for pathways that involve spin-to-triplet transformations.

4. RESULTS AND DISCUSSION

4.1 Adsorption and Dissociation of O, H, O₂, H₂, and H₂O on Al₂O₃ support

Table 3 demonstrates the effect of adsorption and dissociation on the surface reconstruction of the α -Al₂O₃ (0001) surface. Although O₂ and H₂O can molecularly adsorb to surface Al^[1], H₂ cannot. Molecular O₂ adsorbs closer to the surface than H₂O and does not change the contraction of the first inter-atomic layer. In contrast, molecularly adsorbed H₂O causes the surface Al^[1] to contract below the O^[2] atoms, changing the surface termination from Al-terminated to O-terminated although the Al and O atoms are nearly co-planar.

As shown in Figure 4, there are three unique configurations for the dissociated products, henceforth referred to as 1-2, 1-4, and 2-2 dissociation. H₂ can form all three dissociation products. However, H₂O cannot form 2-2 dissociation products and O₂ cannot form 1-4 dissociation products. In comparing the dissociation products, the following trends are clear: (1) dissociation reduces the contraction of the first inter-atomic layer regardless of which species is dissociating and (2) E_{bind} O₂ > E_{bind} H₂ > E_{bind} H₂O. In regards to which type of dissociation product has the lowest energy, it depends on which species are present. For both H₂O and O₂, the lowest energy dissociation products are 1-2. However for H₂, the lowest energy dissociation product is 2-2.

Table3: Effect of Adsorption on Surface Reconstruction.

Note: Layer 1 and Layer 2 are the percent change in the 1st and 2nd inter-atomic layers with respect to their bulk coordinates. A negative sign for Layer1 or 2 represents a contraction of the layer. $\Delta X^{[bind]}$ calculates how much the adsorbate pulls the surface Al^[1] site from its original relaxed position. Al^[1]-O^[2] are the surface bonds neighboring the adsorption site.

	Layer1 (%)	Layer2 (%)	Δ Al ^[1] (%)	Al ^[1] -O ^[2] Å		
Al ₂ O ₃	-89	+6	-----	1.704	1.704	1.704
O (A)	-83	+6	+11	1.783	1.783	1.783
O (B)	-98	+9	+8	1.826	1.715	1.714
H (C)	-87	+6	+11	1.784	1.784	1.784
H (D)	Non uniform		-14	1.841	1.747	1.746
O ₂ (E)	-90	+7	+7	1.735	1.735	1.733
O ₂ (F)	-84	+4	+9	1.878	1.711	1.710
O ₂ (G)	-86	+13	+13	1.869	1.862	1.733
H ₂ (H)	-83	+10	+13	1.920	1.764	1.764
H ₂ (I)	-84	+9	+11	1.796	1.790	1.770
H ₂ (J)	Non uniform		-16	1.844	1.837	1.745
H ₂ O (K)	-104	+6	+6	1.733	1.721	1.720
H ₂ O (L)	-83	+9	+13	1.894	1.755	1.755
H ₂ O (M)	-85	+7	+11	1.793	1.779	1.766
Pt (O)	-95	+5	-18	1.810	1.813	1.816
Pt (P)	-87	+6	-17	1.759	1.817	1.826
Pt (Q)	-83	+3	+8	1.710	1.717	1.799
Pt (R)	-92	+6	+9	1.718	1.719	1.828

4.2 Adsorption of Pt, Pt-O^[ads], Pt₃ on Al₂O₃ support

Atomic Pt can form 4 different structures (Figure 4 O, P, Q, and R) on the α -Al₂O₃ (0001) surface, one that is directly bound to Al^[1] and three different bridging configurations. The directly bound site has the highest energy site (Figure 4O, E_{bind} = -45kcal/mol). In two of the bridging structures (Figure 4Q and R), Pt forms a bridge between Al^[1] and O^[2] pulling the Al^[1] away from the surface whereas in the third, Pt bridges two O^[2] sites and pushes the nearest Al^[1] deeper into the lattice. In general, bridges between Al^[1] and O^[2] sites have lower energy than bridges between O^[2] sites. For the Pt-O^[2] bridging structures, the further the adsorption site is from surface and sub-surface Al, the lower the binding energy and the larger the surface bond angle. One interesting point is that all Pt binding configurations change the local surface termination from aluminum to oxygen terminated. This is likely to have a profound effect on catalytic processes. The barrier calculations performed in section 4.3, all contain Pt as a bridging atom in the #10 binding site. For this binding site, we found three unique Pt-O^[ads] product structures as illustrated in Figure 4 U, V, and W.

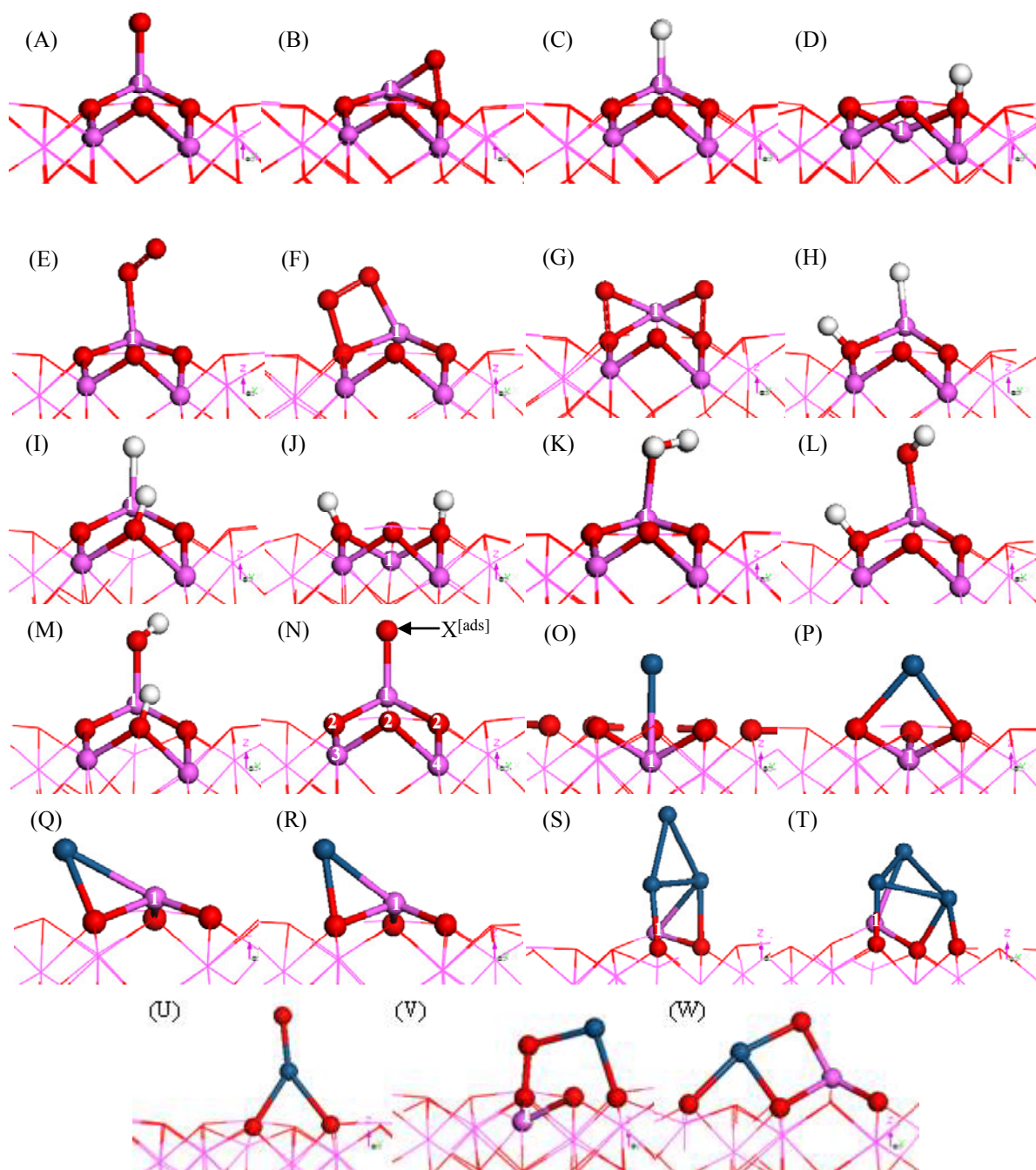


Figure 4: Adsorption and dissociated structures for: (A) Oxygen Tetrahedron (B) Oxygen Bridge (C) Hydrogen Tetrahedron (D) Hydrogen (E) 1-1 Molecularly adsorbed O_2 (F) 1-2 Dissociated O_2 (G) 2-2 Dissociated O_2 (H) 1-2 Dissociated H_2 (I) 1-4 Dissociated H_2 (J) 2-2 Dissociated H_2 (K) 1-1 Molecularly Adsorbed H_2O (L) 1-2 Dissociated H_2O (M) 1-4 Dissociated H_2O (N) Key indicating atomic layer to which atom originally belonged (O) Pt directly bound to $Al^{[1]}$ (P) Pt bridging $O^{[2]}$ (Q) Pt bridging $Al^{[1]}$ and $O^{[2]}$ (R) Pt directly bound to $O^{[2]}$ (S) 90° Pt trimer (T) 37° Pt trimer. (U) O directly bound to Pt bridge (V) O bound as bridge between $O^{[2]}$ and Pt (W) O bound as bridge between $Al^{[1]}$ and Pt. Note for structures U, V, W, the Pt atom was in the #10 binding site before relaxation with the adsorbing O atom.

Pt can also form two different trimer cluster configurations on the $\alpha\text{Al}_2\text{O}_3$ (0001) surface, one that is perfectly perpendicular to the surface ($E_{\text{binding}} = -79$ kcal/mol) and the other that forms a 37° angle ($E_{\text{binding}} = -94$ kcal/mol). Although the surface and internal bonding schemes within the Pt clusters vary with the sub-surface bonding environment, the binding energies are relatively independent. The Pt-Pt binding distance within the cluster is approximately 2.5 to 2.6 Å. As was the case with atomic Pt, Pt trimer clusters also change the local surface termination from aluminum to oxygen terminated.

Table 4: Effect of Local Bonding Environment on the Binding Energies and Bond Lengths for Pt and Pt trimer product structures. The product structures that result from adsorption at sites 0, (4, 16, 14, 5, 6, 9, 10, 13, 15), (3, 7, 11), and (1, 2, 12) are portrayed in Figure 4 as structures O, P, Q, and R respectively.

Pt Adsorption				
Bind site	E_{binding}	$\text{Pt}^{\text{[ads]}}\text{-O}^{\text{[2]}}$	$\text{Pt}^{\text{[ads]}}\text{-Al}^{\text{[1]}}$	\sphericalangle bond
0	-45	-----	2.571	90
1	-59	2.003	2.422	54
2	-59	2.003	2.420	54
12	-59	2.002	2.422	54
4	-50	2.208	2.700	43
14	-50	2.129	2.716	41
16	-50	2.216	2.703	50
5	-53	2.198	3.092	50
6	-54	2.199	2.996	50
9	-53	2.178	3.093	50
10	-62	2.099	3.638	52
13	-60	3.165	2.091	52
15	-60	3.169	2.099	52
3	-60	2.499	2.067	55
7	-60	2.495	2.067	55
11	-60	2.490	2.057	54
Pt Trimer Adsorption				
	E_{binding}	$\text{Pt}^{\text{[ads]}}\text{-O}^{\text{[2]}}$	$\text{Pt}^{\text{[ads]}}\text{-Al}^{\text{[1]}}$	\sphericalangle bond
Figure4S	-79	2.100	2.449	90
Figure4T	-94	2.141	2.527	37

4.3 Surface Diffusion of O towards Pt particle

Table 5 contains the results from the barrier calculations for oxygen surface diffusion towards the catalytically active Pt particle. The presence of Pt decreases the barrier for the diffusion of oxygen in the vicinity of surface $\text{Al}^{\text{[1]}}$ from 27 kcal/mol to 5 kcal/mol. In addition, it induces an exothermic reaction which releases 83 kcal/mol of energy by forming a new product with the Pt particle (Figure 4W). The energetics for diffusion paths that are > 3.7 Å away from the Pt particle are relatively unaffected by the presence of Pt. This is a

preliminary investigation of the effect of surface diffusion and there are still many more pathways and product structures that must be considered before a complete model of oxygen diffusion towards catalytically active Pt particles can be established.

Table 5: Barrier Calculations for Effect of Pt on Oxygen Surface Diffusion

Path ID	With Pt		No Pt	
	E_{barrier} (kcal/mol)	E_{rxn} (kcal/mol)	E_{barrier} (kcal/mol)	E_{rxn} (kcal/mol)
14	4.8	-82.5	26.6	0
10	57.8	-1.6	64.4	0
13	61.7	-4.4	64.4	0
15	69.5	+2.8	64.4	0

5. CONCLUSIONS

In this paper, we identified several adsorption and dissociation products for Pt, $\text{Pt-O}^{\text{[ads]}}$, Pt_3 , O, H, O_2 , H_2 , and H_2O on the $\alpha\text{Al}_2\text{O}_3$ (0001) surface and described how these structures changed the surface reconstruction. Specifically, we concluded that the adsorption of molecular H_2O , atomic Pt, and Pt trimers changed the termination for the $\alpha\text{Al}_2\text{O}_3$ (0001) surface from aluminum to oxygen terminated in the vicinity of the adsorption products. This should have a dramatic affect on catalytic activity and surface diffusion. We confirmed this for O surface diffusion near surface $\text{Al}^{\text{[1]}}$ where the presence of atomic Pt decreased the diffusion barrier from 27 to 5 kcal/mol.

6. ACKNOWLEDGEMENTS

We would like to acknowledge the HPC High Performance Computer Modernization program as well as the thoughtful insights of Dr. Eric Wetzel (US Army Research Laboratory), Dr. Emily Carter (Princeton University) and Ioannis Bourmpakis (University of Delaware).

7. REFERENCES

- Ahn, J. and Rabalais, J.W., 1997: Composition and Structure of the $\alpha\text{Al}_2\text{O}_3$ {0001}-(1x1) Surface, Surf. Sci., **388**, 121-131.
- Alavi, S. Sorescu, D.C., Thompson, D.L., 2003: Adsorption of HCl on Single-Crystal $\alpha\text{Al}_2\text{O}_3$ Surfaces: a DFT Study, J. Phys. Chem. B, **107**, 186-195.
- Carrasco, J., Gomes, J., and Illas, F., 2004: Theoretical Study of Bulk and Surface Oxygen and Al Vacancies in $\alpha\text{Al}_2\text{O}_3$, Phys. Rev. B, **69**, 064116(1-13).
- Delley, B., 2000: From Molecules to Solids with the Dmol3 Approach, J. Chem. Phys., **113**, 7756-7764.

- Delley, B., 2002: Hardness Conserving Semi-Local Pseudopotentials, *Phys. Rev. B*, **66**, 155125(1-9).
- Elam, J.W., Nelson, C.E., Cameron, M.A., Tolbert, M.A., and George, S.M., 1998: Adsorption of H₂O on a Single Crystal α -Al₂O₃ (0001) Surface, *J. Phys. Chem. B*, **102**, 7008-7015.
- Frondelius, P., Hellman, A., Honkala, K., Hakkinen, H., and Gronbeck, H., 2008: Charging of Atoms, Clusters, and Molecules on Metal-Supported Oxides- A General and Long-Ranged Phenomenon, *Phys. Rev. B*, **78**, 085426 1-7.
- Guenard, P., Renaud, G., Barbier, A., and Gautier-Soyer, M., 1998: Determination of α -Al₂O₃ (0001) Surface Relaxation and Termination by Measurements of Crystal Truncation Rods, *Surf. Rev. Lett.*, **5**, 321-324.
- Govind, N., Peterson, M., Fitzgerald, G., King-Smith, D., and Andzelm, J., 2003: A Generalized Synchronous Transit Method for Transition State Location, *Comp. Mat. Sci.*, **28**, 250-258.
- Hass, K.C., Schneider, W.F., Curioni, A. and Andreoni, W., 2000: First Principles Molecular Dynamics Simulations of H₂O on α -Al₂O₃ (0001), *J. Phys. Chem. B*, **104**, 5527-5540.
- Hellman, A. and Gronbeck, H., 2008: Activation of Al₂O₃ by a Long-Ranged Chemical Bond Mechanism, *Phys. Rev. Lett.*, **100**, 1168011-4.
- Herzberg, G., 1950: *Molecular Spectra and Molecular Structure, I. Spectra of Diatomic Molecules*. Van Nostrand Reinhold Company, New York
- Hinnemann, B. and Carter, E., 2007: Adsorption of Al, O, Hf, Y, Pt and S Atoms on α -Al₂O₃ (0001), *J. Phys. Chem. C*, **111**, 7105-7126.
- Kulawik, M., Nilius, N., and Freud, H.J., 2006: Influence of Metal Substrate on the Adsorption Properties of Thin Oxide Layers: Au Atoms on Thin Alumina Film on NiAl(110), *Phys. Rev. Lett.*, **96**, 036103 1-4.
- Marmier, A., and Parker, S., 2004: Ab Initio Morphology and Surface Thermodynamics of α -Al₂O₃, *Phys. Rev. B*, **69**, 115409(1-9).
- Mhadeshware, A. B. and Vlachos, D. G., 2007: A Catalytic Reaction Mechanism for Methane Partial Oxidation at Short Contact Times, Reforming and Combustion, and of Oxygenate Decomposition and Oxidation on Pt, *Ind. Eng. Chem. Res.*, **46**, 5310-5324.
- Miesse, C. et al., 2004: Submillimeter Scale Combustion, *AICHE Journal*, **50**, 3206
- Norton, D. G., Voit, K. W., Bruggemann, T., and Vlachos, D.G., 2004: Portable Power Generation via Integrated Catalytic Microcombustion-Thermoelectric Devices, *Proc. 24th Army Science Conference*.
- Ogawa, S. and Ichikawa, S., 1995: Observation of Induced Dipoles Between Small Palladium Clusters and (0001) α -Al₂O₃, *Phys. Rev. B*, **51**, 17231-17234.
- Perdew, J.P., Burke, K., Ernzerhof, M., 1996: Generalized Gradient Approximation Made Simple, *Phys. Rev. Lett.*, **77**, 3865-3866.
- Ruberto, C., Yourdshahyan, T., and Lundqvist, B., 2003: Surface Properties of Meta-stable Al₂O₃: a Comparative Study of κ and α -Al₂O₃, *Phys. Rev. B*, **67**, 195412(1-18).
- Sousa, C., Illas, F. and Pacchioni, G., 1993: Can Corundum be Described as an Ionic Oxide?, *J. Chem. Phys.*, **99**, 6818-6823.
- Swanson, H.E., Cook, M.I, Evans, E. H. and de Groot, J. H., 1960 Standard X-Ray Diffraction Powder Pattern NBS Circular no 539, 10 (Washington, DC: US Government Printing Office, 3.
- Synowczynski, J., Andzelm, J., and Vlachos, D.G., 2008: Theoretical Investigation of H₂ Combustion on α -Al₂O₃ support, *Proc. 26th Army Science Conference*.
- Verdozzi, C., Jennison, D., Schultz, P., and Sears, M., 1999: Sapphire (0001) Surface, Clean and with d-Metal Overlayers, *Phys. Rev. Lett.*, **82**, 799-802.
- Wang, D., Dewaele, O., and Groote, G. F., 1996: Reaction Mechanism and Role of the Support in the Partial Oxidation of Methane on Rh/Al₂O₃, *J. Catalysis*, **159**, 418-426.